Ability of 24-2C and 24-2 Grids to Identify Central Visual Field Defects and Structure-Function Concordance in Glaucoma and Suspects

JACK PHU AND MICHAEL KALLONIATIS

• PURPOSE: The purpose of this study was to compare the ability of the 24-2 test grid with that of the 24-2C test grid to measure visual field global indices, identify central visual field defects, and facilitate macular structure-function analysis with optical coherence tomography (OCT) scans in glaucoma suspects and glaucoma patients.

• DESIGN: Prospective, cross-sectional study.

• METHODS: One eye from each of 100 glaucoma suspects and glaucoma patients (60 undergoing SITA-Faster [Zeiss Meditec] testing on 24-2 and 24-2C; 40 undergoing SITA-Standard [Zeiss Meditec] testing on 24-2 and SITA-Faster on 24-2C) were included in the study. Global visual field indices, test duration, and pattern deviation results were extracted. The deviation map from the Cirrus OCT (Carl Zeiss Meditec) Ganglion Cell Analysis (GCA) was extracted, and structure-function relationships were compared after correction of the visual field test stimulus location that stimulated the corresponding retinal ganglion cell.

• RESULTS: Global index results of the 24-2 grid were similar to those of the 24-2C grid, and both identified a comparable number of clusters of visual field defects. Centrally, the 24-2C grid identified more clusters of defects than the 24-2 grid, but this was not statistically significant. Although the 24-2C test locations resulted in more instances of structure-function concordance than the 24-2 locations, half the locations in the 24-2C grid fell close to or outside the GCA grid when corrected for ganglion cell displacement.

• CONCLUSIONS: The 24-2C returned global visual field indices similar to the 24-2 grid but tended to identify more clusters of central functional defects. Central structure-function concordance was better achieved using the 24-2C grid, but half of the visual field test locations did not coincide with the commonly used macular thickness scan. (Am J Ophthalmol 2020;219:317–331.

AJO.com Supplemental Material available at AJO.com.

Accepted for publication Jun 18, 2020.

<AFF>From the Centre for Eye Health (J.P., M.K.), University of New South Wales, Kensington, New South Wales, Australia; and the School of Optometry and Vision Science (J.P., M.K.), University of New South Wales, Kensington, New South Wales, Australia.

Inquiries to Jack Phu, Centre for Eye Health, University of New South Wales Sydney, Gate 14 Barker Street, Rupert Myers Building, South Wing, 2052 New South Wales, Australia; e-mail: jack.phu@unsw.edu.au

ASSESSMENT OF THE VISUAL FIELD USING PERIMETRIC testing is a key clinical procedure in patients with suspected or diagnosed glaucoma.[1,2] The test grid and number of test locations have been subjects of investigation to optimize detection of visual field defects arising from glaucoma.[3,4] Common clinical acumen dictates the need to strike a balance between the number of test locations required for adequate decision making while making the test of a practical length for the patient and examiner.[5] It is also desirable for test grids to assess the same test locations to facilitate a comparison between results, as in progression analysis.[6]

With respect to static automated perimetry, there is a divide between grids biased toward assessing the more peripheral visual field and those tending toward the central visual field.[7–10] Due in part to its prolific use in clinical trials and its ability to assess a broad extent of the visual field relevant for detecting glaucoma-related visual field defects, the more "peripheral" 24-2 or 30-2 (or similar) grid has become the clinical standard for glaucoma assessment.[11–14]

Using the 24-2 in isolation has been challenged by studies reporting on the prevalence of central visual field defects not typically detected by the 24-2 test grid. Instead, spatially dense central test grids, such as the 10-2, have been proposed to map out central scotomata.[7,8,15] Studies investigating neural losses occurring within the macula region in glaucoma have highlighted the need to sample and map out central visual function.[16] Identification of central visual field loss is relevant for a number of glaucoma severity staging systems and, hence, have relevance in treatment titration.[17] Depending on the individual, vision loss in the central field may adversely affect necessary daily functions and quality of life.[18]

Issues pertaining to switching among test grids stem from the incompatibility of mixing grids for progression analysis

and the impracticalities of conducting both in a single clinical visit, given that many clinics are unable to complete one test per visit.[19] To address these issues, modifications to the existing test grids have been proposed, such as the addition of test points to the existing 24-2 or similar to create a combined grid assessing both central and peripheral fields.[20,21]

Recently, the 24-2C has become available for clinical use on the Humphrey field analyzer (Carl Zeiss Meditec, Dublin CA), which incorporates 10 additional test points within the central 10° from fixation, 5 in each hemifield. Unlike the rest of the test grid and the 10-2 grid, the additional points are not symmetrically distributed across the vertical or horizontal midlines. The locations of the test points were purportedly derived from test locations commonly affected in glaucoma, but the usefulness of these points has yet to be tested. Another potential practical advantage of deploying the 24-2C grid is that sensitivity measurements are driven by the SITA-Faster paradigm (Carl Zeiss Meditec, Dublin, CA), which reduces test time by around 50% from the conventionally used SITA-Standard (Carl Zeiss Meditec, Dublin, CA).[22,23]

Despite the implementation of strategies designed to address current shortcomings in clinical perimetry for glaucoma, the performance of the 24-2C has yet to be formally and independently assessed in comparison to the 24-2 grid, which is the current clinical standard for conditions such as glaucoma. Furthermore, it has not yet been correlated with structural measurements of the central macular region, obtained using imaging modalities such as optical coherence tomography (OCT). Thus, the purpose of the present study was to assess the clinical utility of the 24-2C grid. There were 3 aims to this study. First, the resultant global indices and conventional clinical outcomes (mean deviation, pattern standard deviation, and identification of clusters of visual field loss) were examined. The purpose of this was to identify systematic differences that might exist in indices commonly used in glaucoma assessment.[24] Second, the test durations were compared between grids, and the issue of whether the additional points might incur a significant time disadvantage was investigated. The question there was to determine the tradeoff that might be required for additional information in the central visual field. Finally, the performance of the conventional 24-2 test grid and the additional 10 points in detecting visual field defects concordant with statistically significant structural losses using the macular (ganglion cell-inner plexiform layer thickness) scan protocol on an OCT instrument provided by the same manufacturer were assessed and compared.

METHODS

• **STUDY DESIGN AND SUBJECTS:** This study was a prospective, cross-sectional study. Ethics approval for the study was provided by the Human Research Ethics Committee of the University of New South Wales. The study adhered to the tenets of the Declaration of Helsinki. Subjects provided written informed consent prior to inclusion in the study.

The study took place at the Centre for Eye Health, University of New South Wales. Patients seen at the Centre for Eye Health had been referred for glaucoma assessment by external eye care practitioners. For this study, patients were prospectively identified and recruited to undergo testing using both the 24-2 and 24-2C test grids. All patients were existing patients at the Centre for Eye Health and had experience undertaking perimetric testing.

Patients with glaucoma or high-risk glaucoma suspects were specifically targeted.[25,26] Glaucoma was diagnosed according to current clinical guidelines, including clear characteristic glaucomatous structural anomalies at the optic nerve head (including but not limited to increased cup-to-disc ratio, cup-to-disc asymmetry, and neuroretinal rim thinning or notching), and/or retinal nerve fiber layer (corresponding to the aforementioned neuroretinal rim changes), with or without corresponding visual field loss (defined using the 24-2 SITA-Standard result, consisting of a pattern standard deviation result at $P < .05$, a Glaucoma Hemifield Test result outside normal limits or a "fail" on the cluster criterion (described below), and with or without elevated intraocular pressure.[27] Patients suspected of having glaucoma were those in whom one or more of the above signs were present but where the signs were insufficient for a diagnosis of glaucoma requiring therapeutic intervention. Glaucoma was clinically diagnosed by at least one examining clinician, with remote review by at least one other clinician. For the patient to be included in the study, the diagnosis was also agreed upon by a third clinician.

Other inclusion criteria included age 18 years or older; provided consent to use of their clinical data for research and teaching; no other ocular, systemic or neurological comorbidities that would confound the visual field test result; no history of ocular surgery aside from uncomplicated selective laser trabeculoplasty, laser peripheral iridotomy, or cataract surgery and intraocular lens implantation; no history of ocular trauma; spherical equivalent refractive error between +8.00 diopters (D) and −8.00 D; and the inability to complete a perimetric test.

• **VISUAL FIELD TESTING AND DATA EXTRACTION:** Patients underwent testing by using both the 24-2 and the 24-2C grids. In all instances, the 24-2 test grid was examined first, followed by the 24-2C grid. A random eye was chosen for testing.

Two cohorts of patients were tested. In the first cohort, patients underwent testing using the 24-2 grid with the SITA-Standard paradigm, followed by testing using the 24-2C grid with the SITA-Faster algorithm. In the second cohort, patients underwent testing using both the 24-2 and the 24-2C with SITA-Faster. The reason for this was to

examine whether systematic differences existed between the manner in which central test points were evaluated using SITA-Standard or SITA-Faster and how this might relate to 24-2C testing. Tests were performed on the same day, and the perimetrist was instructed to provide adequate rest breaks between tests to mitigate the potential contribution of fatigue.

The reliability criteria for inclusion in the present study were a false positive rate below 15%; no seeding point errors[28]; <20% of instances where the gaze tracker deviation exceeded 6° during the test; and the absence of other technician-related errors (including incorrect trial lens usage, lens rim artifacts, poor patient position, and others). Elevated rates of false negatives and fixation losses using the Heijl-Krakau method were not used as measurements of low test reliability, as both are poor indicators of true reliability, confounded by the presence of disease and anatomical variation, and because we wished to directly compare the SITA-Standard and SITA-Faster algorithms (in the latter, false negatives and blind spot monitoring were turned off by default).

The total sample of patients undergoing SITA-Faster 24-2 and 24-2C was 117. Within this group, 60 had reliable results on both tests (51.3%). Of the remaining, 20 patients (17.1%) had unreliable results on both; 17 patients (14.5%) had reliable results on the 24-2 grid only; and 20 patients (17.1%) had reliable results on the 24-2C grid only. A total of 61 patients underwent testing on SITA-Standard 24-2 and SITA-Faster 24-2C grids, of which 40 had reliable results on both patterns (65.6%). Of the remaining, 9 patients (14.8%) had unreliable results on both; 8 patients (13.1%) had reliable results on the 24-2 grid only using SITA-Standard; and 4 patients (6.6%) had reliable results on the 24-2C grid only. There were no differences in the distribution of reliability among test grids between SITA-Faster and SITA-Standard ($P = .2447$).

• **AIM 1: COMPARISON OF CONVENTIONAL VISUAL FIELD INDICES:** Mean deviation, pattern standard deviation, and the glaucoma hemifield test have been used and widely reported as markers of potential visual field loss in glaucoma and for disease staging (and hence treatment titration). Both the 24-2 and 24-C report on these indices, so their results were compared for each patient. The mean sensitivity of the test points within the central 10-degrees across test grids (12 locations in the 24-2 and 22 locations in the 24-2C) were also compared. However, the exact weighting of these test locations and their post-test modulations are not precisely known; hence, first the antilog of the decibel value was taken from the total deviation plot, then the result was averaged before it was finally converted back to a mean decibel unit, according to the method of Hood and Kardon.[29] The result for each subject was considered the central mean sensitivity.

Another index of statistically significant visual field loss is the "cluster" criterion. This study used the definition of a group of 3 or more contiguous points of statistically significant reduction in sensitivity (at least 3 points at the P level $<.05$), where at least 1 point is at the P level of $< .01$ level) noted in the pattern deviation map. This was a binary outcome in terms of whether a visual field result did not meet (passed) or met (failed) the criterion. Further to the "cluster" criterion, it was also noted whether the 24-2C grid was additive to the pass/fail outcome. If a visual field result using 24-2 grid points demonstrated a fail on the "cluster" criterion, then the contribution of the 24-2C to this visual field outcome would be regarded as nonadditive. If the 24-2 only points were insufficient for identifying a "cluster" fail and that the criterion was only met through the contribution of the 24-2C, then it would be regarded as additive. Note that, due to the asymmetric distribution of the additional 10 points of the 24-2C, the contiguity rule noted above was applied for any adjacent point within the grid.

The aim of the criterion described above was to identify statistically significant clusters that were typically used in the glaucoma assessment, and the 3 or more contiguous points requirement operates within a symmetrical test grid. However, the application of this criterion within the central visual field translates to potentially unequal retinal ganglion cell stimulation.[30] Therefore, this criterion may not be suitable for central locations, so we also assessed the number of occasions where at least 2 contiguous (with the product of P level of $\leq.00025$) points or at least 1 solitary point (at least at the P level of $<.0001$) identified as abnormal within the central 10-degrees of the visual field (12 points in the 24-2; 22 points in the 24-2C).The P value criteria were set to be as close as possible to the conventional "three or more points" criterion described above and practically identified by the perimeter. The frequency of occurrence was compared across grids.

• **AIM 2: COMPARISON OF TEST DURATION:** The addition of 10 points to the test grid is expected to increase the test duration. Thus, although it may add clinical information, the perceived benefits should be weighed against the cost of time incurred with more numerous points. Thus, the second aim was to compare the test durations obtained using the different test grids. Although the 24-2C test grid presents stimuli at the 10 additional locations after the 54 test locations of the conventional 24-2 grid have been assessed, the final test duration reported in the results represents the total test time, hence we did not isolate the time specifically related to the 24-2C exclusive locations.

• **AIM 3: COMPARISON OF COLOCALIZED STRUCTURAL AND FUNCTIONAL CENTRAL DEFECTS:** Given that a goal in glaucoma assessment is to achieve structure-function concordance, the third aim was to examine the ability of the conventional 24-2 test grid and the 24-2C grid to detect colocalized structural and functional losses

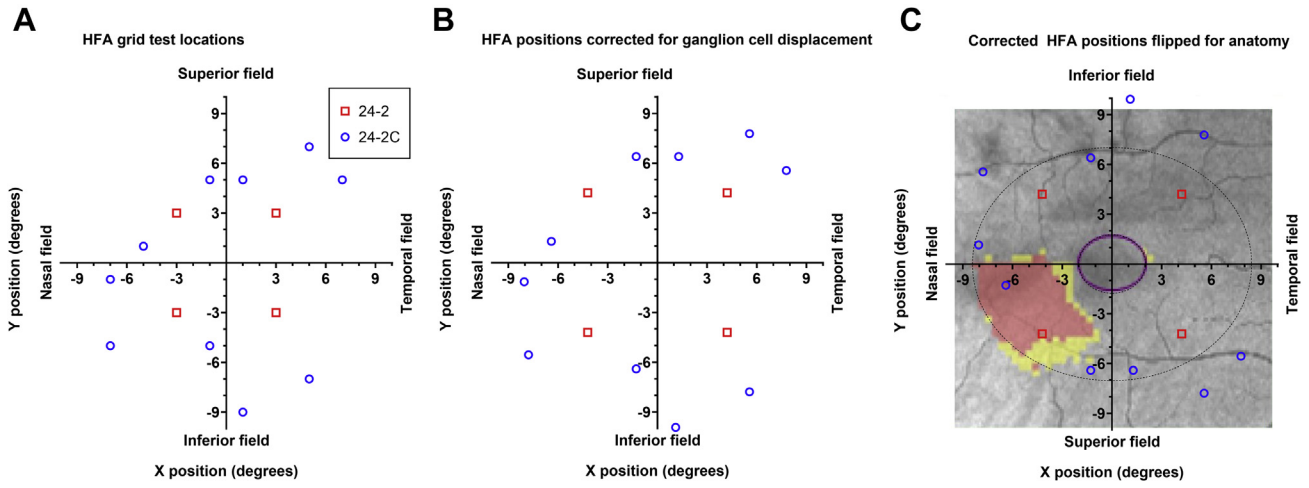

FIGURE 1. (A) Humphrey field analyzer (HFA) was used for central visual field test positions for the 24-2 (red squares) and the exclusive 24-2C points (blue circles) for a right eye. (B) HFA test locations after adjusting for ganglion cell displacement. (C) HFA test locations after adjusting for ganglion cell displacement and inverted for structure-function correlations with retinal anatomy. The visual field test grid has been inverted (superior field in the inferior anatomical position) and is superimposed on a ganglion cell analysis deviation map obtained from Cirrus optical coherence tomography. The dashed black line indicates the boundary of the ganglion cell analysis deviation map and the structure-function correlations were performed within this boundary.

within the central visual field. In order to test the purported advantages of the 10 points added to the 24-2C, the 4 centrally located points within the 24-2 (Cartesian coordinates 3.3-degrees from fixation in each quadrant) were compared to the 10 points exclusive to the 24-2C (Figure 1, A). The projected retinal positions of these test locations were corrected to account for the relative displacement of Henle's fibers,[31] according to previously described methods (Figure 1, B).[30,32] These positions were then superimposed on macular OCT scans (macular cube 512 × 128 scanning protocol), segmenting the ganglion cell inner plexiform layer thickness values, the ganglion cell analysis printout of the Cirrus OCT (Carl Zeiss Meditec, Dublin, California). The ganglion cell analysis provides ganglion cell inner plexiform layer thickness values within an elliptical annulus measuring 14.13 mm^2, with vertical inner and outer radii of 0.5 and 2.0 mm and horizontal inner and outer radii of 0.6 and 2.4 mm, respectively. This translates to dimensions of approximately 7- × 8.4-degrees (Figure 1, C dashed oval). We chose to perform the structure-function correlations using the OCT device from the same manufacturer as the perimetry results.

Although in clinical practice both the retinal nerve fiber layer and macular scans (or similar combinatory protocols) are recommended for use in the glaucoma assessment, for the purpose of this study, the macula scan alone was the focus for several reasons. The Cirrus OCT provides measurements of retinal nerve fiber layer thickness (optic nerve head scan protocol), and the structure-function relationship has been reported to differ from that of ganglion cell inner plexiform layer thickness measurements. This is due to the need to account for retinal nerve fiber layer projections, which may differ across individuals, and their localization typically requires a specific, high-resolution scan protocol.[33] The projections are affected by the optic nerve head position relative to the fovea, and the tilt of these structures contributes to the need to modify the correlation with the fixed visual field test grid[34] (see Discussion).

To account for variations in patients ages, statistically significant reductions in visual field sensitivity were compared and retinal thickness, that is, the Humphrey field analyzer pattern deviation map was superimposed (flipped along the horizontal axis to account for retinal projection and accounting for ganglion cell displacement) results upon the ganglion cell analysis deviation map (Figure 1, C). The test grids analyzed were the 24-2, the 24-2 component extracted from the 24-2C, and the 24-2C only points. For these analyses, visual field test locations were considered showing a P value of $<.05$ to be statistically significant. Similarly, deviation map results at a P value of $<.05$ were considered to be statistically significant. The test locations were noted as one of the following: "neither," signifying neither structure nor function demonstrating a reduction; "both," "structure" only; or "function" only. In addition to this condition, a more stringent visual field condition was applied to account for potential differences in measurement variability with a P value $<.01$ on perimetry required to match a P value $<.05$ structural loss (a P value of $<.10$ was not used for the OCT result[35] as the ganglion cell analysis at minimum identifies defects at the level of $P<.05$).

• **STATISTICAL ANALYSIS:** We used descriptive statistics to analyze the demographic characteristics of the cohorts. The distributions of quantitative data were first assessed

TABLE 1. Characteristics of Patients Showing Reliable Results on both 24-2 and 24-2c for the 2 Cohorts in the Present Study

	SITA-Faster (n = 64)	SITA-Standard (n = 40)
Median age (IQR) [a]	62.0 (52.75, 69.0)	59.0 (52.0, 67.8)
Median spherical equivalent refractive error (IQR)[a]	0.00 (−2.25, +0.78)	+0.13 (−1.47, +1.69)
Sex[b]		
Males	37 (57.8)	22 (55.0)
Females	27 (42.2)	18 (45.0)
Eyes [b]		
Right	35 (54.7)	21 (52.5)
Left	29 (45.3)	19 (47.5)
Ethnicity [b]		
White	42 (65.6)	26 (65.0)
Asian	20 (31.2)	13 (32.5)
Indian	2 (3.1)	1 (2.5)
Diagnosis [b]		
Glaucoma	42 (65.6)	19 (45.0)
Suspect	22 (34.4)	21 (55.0)

IQR = interquartile range.
[a]No significant differences were found using the Mann-Whitney *U* test ($P > .05$).
[b]No significant differences were found using the Fisher exact test ($P > .05$).

for normality using a D'Agostino and Pearson test of normality, with parametric and nonparametric statistics then applied as appropriate. For analyses comparing 2 groups, we used either a *t*-test or a Wilcoxon test (confidence intervals [CI] determined at 95%, or as near as possible for nonparametric methods for median differences [see below]). For analyses with more than 3 groups, a one-way ANOVA or a Kruskal-Wallis test was used. The Fisher exact test or chi-squared test was used to assess proportional data, except for the structure-function colocalization, which was assessed using a McNemar test for the quantitative values. Analyses were conducted using Prism version 8 software (GraphPad, La Jolla, California).

RESULTS

• **DEMOGRAPHIC AND CLINICAL CHARACTERISTICS OF COHORTS:** The characteristics of the patients with reliable results on both grids that were finally included in this study are shown in Table 1. There were, overall, no differences in the distributions of age, sex, ethnicity, or refractive error between SITA-Faster and SITA-Standard cohorts. Although there were more glaucoma patients in the SITA-Faster cohort who met study inclusion criteria, this did not reach statistical significance.

• **AIM 1: COMPARISON OF CONVENTIONAL VISUAL FIELD INDICES:** Comparisons were made among mean deviation, pattern standard deviation, and glaucoma hemifield test outcomes between the 24-2 and 24-2C grids (Figure 2). For the SITA-Standard cohort, the average mean deviation result was found to be worse using the 24-2C grid (median difference, −0.73 dB; 96.2% CI, −1.01 to −0.06 dB; $P = .0038$), but there were no significant differences for the SITA-Faster cohort (median difference, −0.02 dB; 96.7% CI, −0.33 to 0.30 dB; $P = .9715$). The pattern standard deviation and glaucoma hemifield test results were not significantly different between the test grids. Central mean sensitivity was also worse for the 24-2C grid than for the 24-2 grid for the SITA-Standard cohort (median difference, −0.35 dB; 96.2% CI, −0.70 to 0.03 dB; $P = .0226$) but was not significantly different between the grids for the SITA-Faster cohort (median difference, −0.13 dB; 96.7% CI, −0.27 to 0.04 dB; $P = .2769$).

Then the number and clusters of statistically significant sensitivity reductions were assessed across the test grid (Figure 3). Considering a binary "failed" cluster criterion (see Methods), there were no significant differences among 24-2 only, 24-2C (all), and 24-2C (24-2 component only) for both the SITA-Standard and the SITA-Faster cohorts (Figure 3). From this analysis, there were no cases where the 24-2C identified a visual field defect cluster that was not found with the 24-2 grid using SITA-Standard. In the SITA-Faster cohort, there were 2 cases (2 of 64 [3.1%]) in whom the 24-2C grid found a statistically significant cluster of defects not identified by using the 24-2 grid only.

The presence of central visual field defects (using 1+ solitary, 2+ contiguous, or 3+ contiguous points of reduction) was compared across test grids. Although there was a

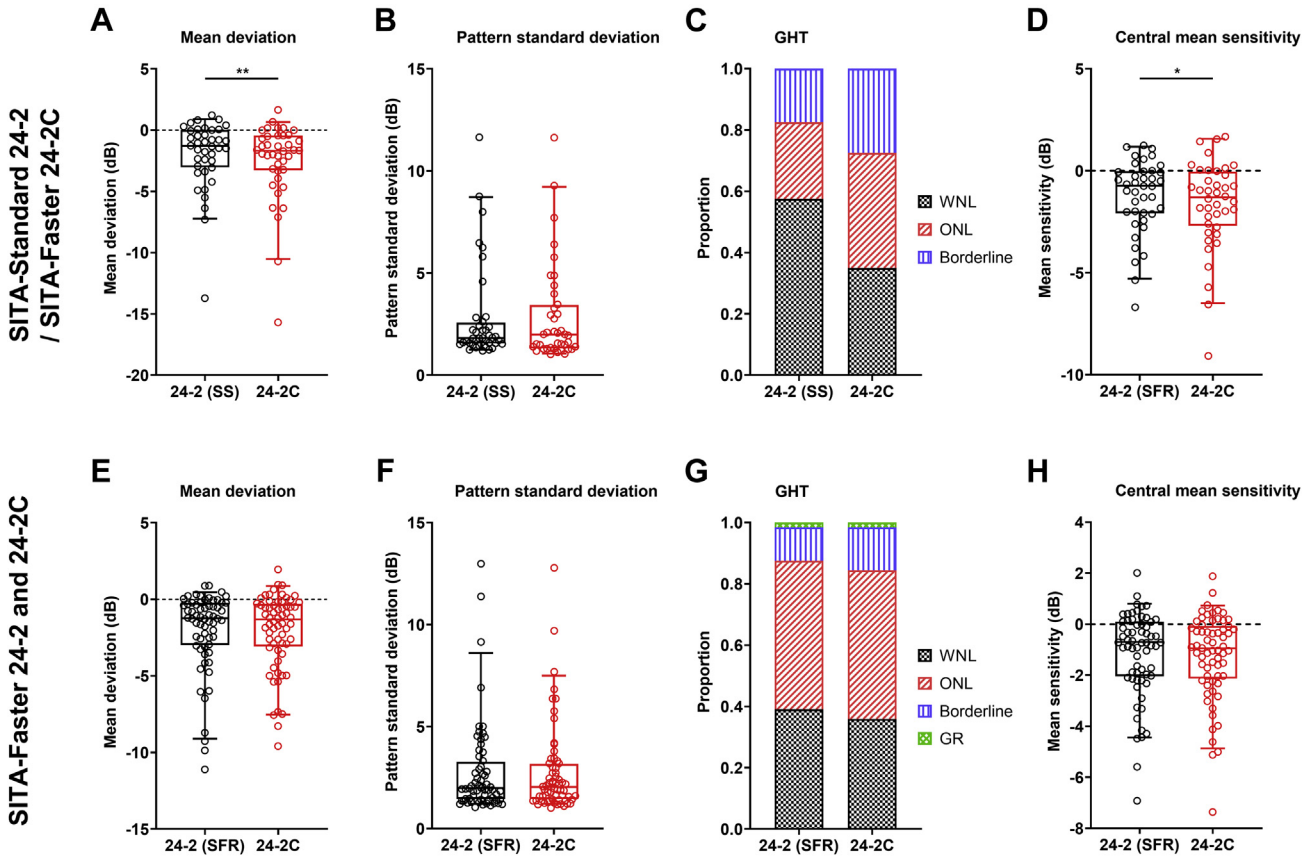

FIGURE 2. Mean deviation pattern (left column, A and E) standard deviation (middle column, B and F) and glaucoma hemifield test (GHT, right column, C and G) results for 24-2 and 24-2C test grids. In addition, central mean sensitivity (as described in the text) was compared between the grid patterns (D and H). The cohort undergoing SITA-Standard 24-2 and SITA-Faster 24-2C testing is shown in the top row, and the cohort undergoing SITA-Faster testing for both grids is shown in the bottom row. To distinguish between the 24-2 thresholding algorithm, the 24-2 SS indicates testing using SITA-Standard and 24-2 SFR indicates testing using SITA-Faster. The asterisks indicate a statistically significant difference between 24-2 and 24-2C results ($P < .01$). SITA = Zeiss Meditec product designation.

tendency for more clusters to be identified by the 24-2C only grid than by the 24-2 only grid, the McNemar test results revealed no significant differences between the 24-2C and 24-2 in identifying central clusters of reduction for all criteria (Figure 3).

• **AIM 2: COMPARISON OF TEST DURATION:** Due to algorithm differences, the test duration for SITA-Standard 24-2 (median, 314.0; interquartile range [IQR], 283.8, 338.0 seconds) was longer than the SITA-Faster 24-2C (median, 155.0; IQR, 140.0, 174.0 seconds), with a median difference of −153.5 seconds (96.2% CI, −164.0 to −141.0 seconds; $P < .0001$) (Figure 4, A). Similarly, due to the additional points assessed in the 24-2C grid, duration for this test grid (median, 154.5; IQR, 136.3, 181.8 seconds) was longer than the conventional 24-2 SITA-Faster (median, 125.5; IQR, 110.5, 148.8 seconds), with a median difference of 26 seconds (96.7% CI, 22.0-31.0 seconds; $P < .0001$) (Figure 4, B).

• **AIM 3: COMPARISON OF COLOCALIZED STRUCTURAL AND FUNCTIONAL CENTRAL DEFECTS:** The proportion of points at which defects occurred on structural (ganglion cell analysis at the $P < .05$ level) and functional (pattern deviation map at the $P < .05$ level and the more stringent $P < .01$ level) tests were compared across the different test grids (Table 2). The locations of interest here were the ganglion cell analysis anatomical locations underpinning the Humphrey field analyzer test locations after accounting for ganglion cell displacement (see Methods). For all test grids and both SITA-Faster and SITA-Standard with both at the $P < .05$ level there were more instances in which structural defects were identified exclusively compared to exclusively functional defects (at least $P = .0228$ for all). Considering the differences in frequency, the 4 points of the 24-2 component identified 4.5- to 12.7-times fewer instances of functional defects than structural defects, whereas the 24-2C identified only 1.6- to 2.0-times fewer cases ($P < .0001$). As expected, this was also

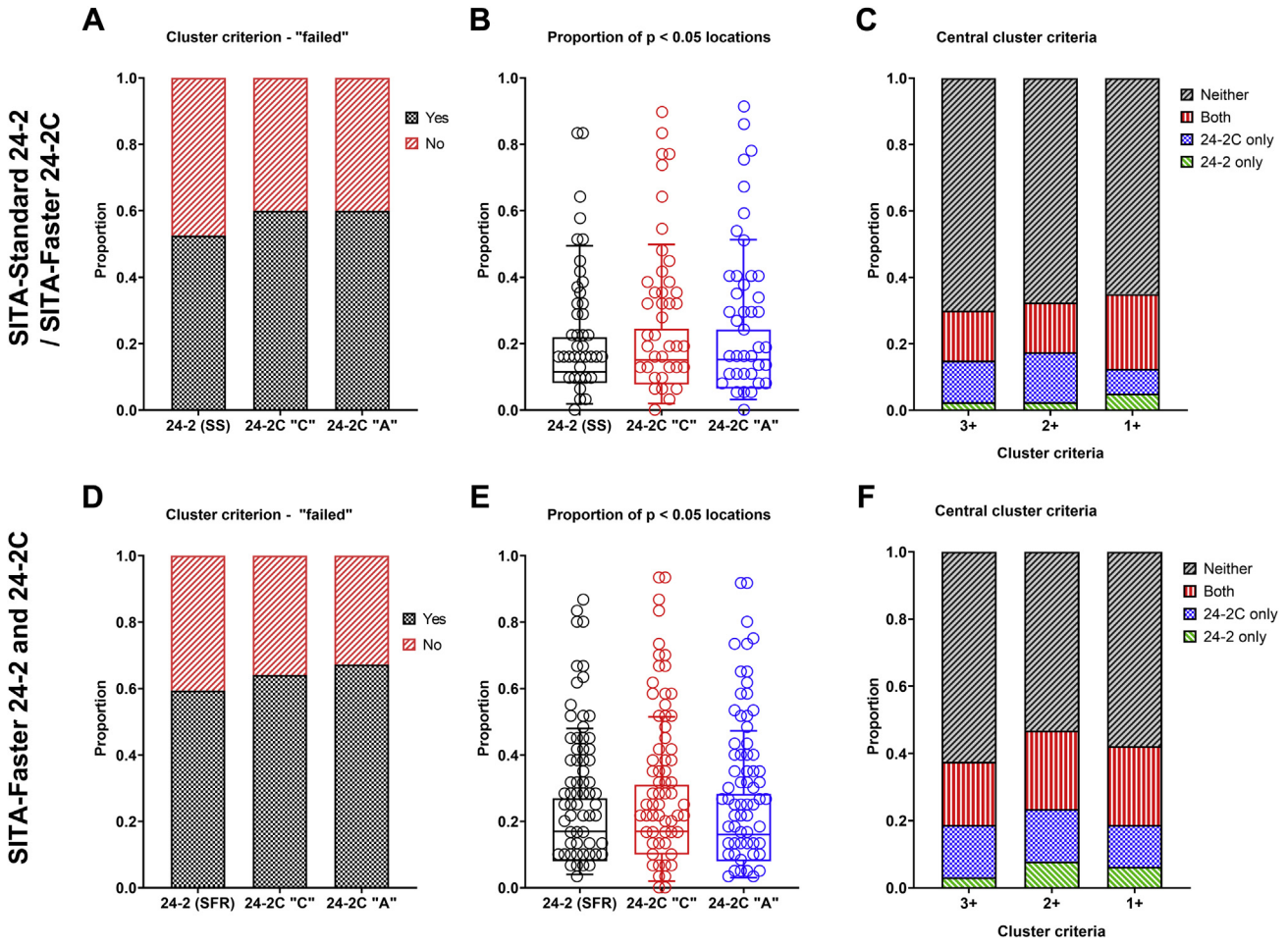

FIGURE 3. Results of analyzing the cluster criterion outcome in the visual field. A "fail" represents the presence of a cluster of 3 or more contiguous points of statistically significant reduced sensitivity ($P < .05$; at least 1 of which is at $P < .01$ level). (A, D) Results when considering if a "fail" was noted in the result. (B) (E) Scatter and box-and-whisker plots (median, interquartile range and 5th to 95th percentile) show the proportion of test points for each grid at which there were statistically significant reductions in sensitivity (at least $P < .05$). Each datum point indicates the result for an individual patient. The x-axis labels indicate the grid conditions: the 24-2 grid (SS = SITA-Standard; SFR = SITA-Faster), 24-2 component of the 24-2C (24-2C "C"), and all of the 24-2C (24-2C "A"). (C, F) Results of the central cluster "fail" criteria (see Methods). (C, F) Number of contiguous (3+ or 2+) or solitary (1+) points of significant reduction. The different colors indicate the conditions under which the central cluster criteria demonstrated a "fail."

evident when a stringent $P < .01$ criterion was used for functional defects ($P < .0001$ for all).

After noting that many locations had neither structural nor functional defects and that there was a propensity for more structural defects to be identified, locations were compared at which structural defects were noted, and the ability for each test grid to identify those defects was compared (Table 3). Pairwise comparisons for the SITA-Standard cohort showed no significant differences in performance between the 24-2 or 24-2C test grids. For the SITA-Faster cohort, the 24-2C test grid identified more significant defects at regions with structural loss than the 24-2 grid. A similar tendency was found with the more stringent $P < .01$ criterion was used.

The relative frequency at which individual visual field test locations were identified was also examined (Table 4). The frequency of defects identified across all locations when considering a criterion where any functional deficit was present for the 24-2 locations was not significantly different ($P = .2270$ for SITA-Standard and $P = .5309$ for SITA-Faster). For 24-2C test locations, the frequency of functional defects identified across locations in the SITA-Standard cohort were not significantly different ($P = .6310$), but there were significant differences in the distribution in the SITA-Faster cohort ($P = .0349$).

The same analysis performed for visual field test locations demonstrating an underlying structural defect showed significant differences in the frequency of defect occurrence

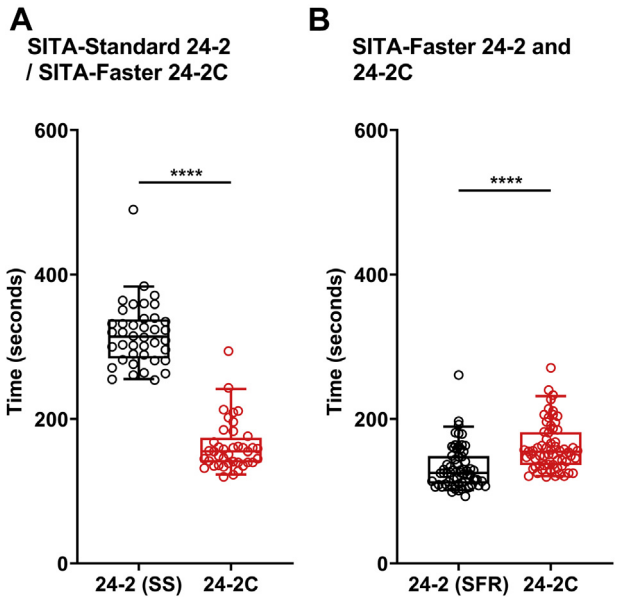

FIGURE 4. Test durations for the 24-2 and 24-2C test grids for the cohort undergoing SITA-Standard 24-2 and SITA-Faster 24-2C (A) and SITA-Faster for both 24-2 and 24-2C (B). Box-and-whiskers plot indicate the median, interquartile range and 5th to 95th percentiles, and each datum point indicates the result for an individual patient. Distinction is made between the 24-2 thresholding algorithm, the 24-2 SITA-standard and 24-2 SITA-Faster. The asterisks indicate statistically significant differences between grids (**, $P < .0001$).**

for all conditions ($P < .0001$) (Table 4). Despite the preponderance for more structural losses to be identified than functional losses, there were also locations at which no structural defects were seen, specifically at anatomical locations (Table 4, annotated 4, 5, 7, 9, and 10). These locations corresponded to those that fell outside the ganglion cell analysis scan circle after accounting for ganglion cell displacement (Figure 1).

DISCUSSION

THE PRESENT STUDY SOUGHT TO EVALUATE THE PERFORmance of the recently commercially available 24-2C test grid using SITA-Faster for the identification of central visual field defects relative to the 24-2 (using either SITA-Standard or SITA-Faster). Global indices of visual field results were similar between the 2 test grids. When colocalized structural defects were considered, the 24-2C clearly identified more locations exhibiting structure-function concordance than the 24-2, but half of all locations were not colocalized. The tradeoff for identifying more defective locations in the central visual field was an increase in test time of approximately 20-30 seconds in comparison to the 24-2 which used the same thresholding algorithm, SITA-Faster.

• **TEST DURATION AND VISUAL FIELD INDICES USING 24-2C COMPARED TO THE 24-2:** Currently, no other independent studies have compared the utility of the 24-2C to other commonly used test grids on the Humphrey field analyzer. Reports of the 24-2C have been largely limited to those produced by the manufacturer. The manufacturer-sponsored studies, however, remain useful for comparison with the present results.

The prolongation of test duration found in the present subjects was slightly longer than that reported by Yu and associates (Yu S, et al. ARVO E-Abstract, 2019;60:2454, Vancouver, BC) comparing 24-2 with 24-2C test grids assessed using SITA-Faster (approximately 25% in the present study compared to approximately 18% in the study by Yu and associates). Given the overall test duration of less than 2 minutes, this percentage difference would translate to approximately 8.5 seconds, which is unlikely to be clinically significant.

By extracting the comparisons of mean deviation results reported by Lee and associates (Lee GC, et al. ARVO E-Abstract, 2019;60:2455, Vancouver, BC), we were able to compare our results to theirs with specific regard to glaucoma patients. In comparison to the study by Lee and associates, whose distribution of mean deviation results for SITA-Standard, SITA-Faster 24-2, and SITA-Faster 24-2C showed no significant differences in the glaucoma group, a statistically significant worse result was found, using the 24-2C in comparison to SITA-Standard. However, similar to test time, the median difference of −0.73 dB was unlikely to be clinically significant. Therefore, when considering global indices that may be used clinically, the 24-2C offers quantitative measurements similar to those of the clinical standard 24-2 test grid. Additionally, assessment of central mean sensitivity found a tendency (difference of 0.13 dB for SITA-Faster and 0.35 dB for SITA-Standard) similar to the mean deviation, reinforcing the present finding that quantitative global indices were not clinically significantly different between test grids.

In their evaluation of the 24-2C, Callan and associates (Callan T, et al. ARVO E-Abstract, 2018;59:5111, Honolulu, Hawaii) counted the number of statistically significantly depressed points on the total and pattern deviation maps. If the absolute number of reduced points are considered, then the 24-2C exclusive test locations would certainly be additive to the 24-2 grid. The present approach instead was to quantify the proportion of reduced points and, in doing so, assess whether some points may be spurious in their contributions to central visual field testing. One findings was that, for the majority of patients, the additional test points in the 24-2C did not add further statistically significant clusters (3 or more contiguous points) of sensitivity reductions, that is, not contributing to a criterion where a visual field result may be considered

TABLE 2. Comparison of Humphrey Field Analyzer and Cirrus OCT Ganglion Cell Analysis for Each Test Grid[a]

	SITA-Faster 24-2 and 24-2C Cohort			SITA-Standard 24-2 and SITA-Faster 24-2C cohort		
	Structure (Ganglion Cell Analysis)			Structure (Ganglion Cell Analysis)		
	Yes	No	*P* Value	Yes	No	*P* Value
Functional defects at $P < .05$						
24-2 test grid						
Yes	12 (4.7)	8 (3.1)	<.0001	10 (6.3)	5 (3.1)	<.0001
No	87 (34.0)	149 (58.2)		51 (31.9	94 (58.8)	
24-2C test grid (24-2 component only)						
Yes	10 (3.9)	7 (2.7)	<.0001	10 (6.3)	11 (7.1)	<.0001
No	89 (34.8)	150 (58.6)		51 (31.9)	88 (55.0)	
24-2C test grid (24-2C component)						
Yes	28 (4.4)	70 (10.9)	<.0001	21 (5.3)	39 (9.8)	.0228
No	128 (20.0)	414 (64.7)		63 (15.8)	277 (69.3)	
Functional defects at $P < .01$						
24-2 test grid						
Yes	6 (2.3)	2 (0.8)	<.0001	7 (4.4)	1 (0.6)	<.0001
No	93 (36.3)	155 (60.5)		54 (33.8)	98 (61.3)	
24-2C test grid (24-2 component only)						
Yes	4 (1.6)	2 (0.8)	<.0001	8 (5.0)	6 (3.8)	<.0001
No	95 (37.1)	155 (60.5)		53 (33.1)	93 (58.1)	
24-2C test grid (24-2C component)						
Yes	18 (2.8)	30 (4.7)	<.0001	16 (4.0)	18 (4.5)	<.0001
No	138 (21.6)	454 (70.9)		68 (17.0)	298 (74.5)	

[a]Table data compare colocalization of statistically significant functional (Humphrey field analyzer at both $P < .05$ and $P < .01$) and structural (Cirrus OCT ganglion cell analysis at $P < .05$) defects for each test grid. Defect present is indicated by "Yes" and no defect present is indicated by "No." The number of cases is shown with the percentage of total in parentheses. The *P* values for the pairwise McNemar tests are shown.

glaucomatous, in comparison to the conventional 24-2. It was noted that this particular "cluster" criterion is related to the entirety of the 24-2 test grid, which has a symmetrical distribution of equally spaced (along the x- and y-axes) locations, unlike the 24-2C exclusive points, so the frequency of central test location sensitivity reduction was also compared. There was a tendency for the 24-2C to identify clusters of sensitivity reduction within the 10° compared to the 24-2 test grid alone. Although this was not found to be statistically significant, this highlights the potential role for an increased index of suspicion for central field loss for the examining clinician. These results also identify the need to revise classic glaucoma visual field diagnostic criteria, which may underestimate the extent of functional loss, by incorporating extra central visual field information.

Overall, the results show little difference in visual field global indices between 24-2 and 24-2C, but highlight several key points that demonstrate an approximately 4-fold greater frequency of colocalized structural defects when using the 24-2C and identification of central defects. Although there is a cost of approximately 20-30 seconds compared to the 24-2 when using SITA-Faster, there is the potential advantage of alerting the clinician to the presence of central visual field loss. Potentially, understanding the characteristics of central visual field loss may assist in developing grids specifically for structure-function correlations within this region.

• **DERIVATION OF USEFUL POINTS FOR TESTING THE CENTRAL VISUAL FIELD:** In comparison to the 10-2, the 24-2C test grid uses a subset of points that are asymmetrically distributed between the superior and inferior hemifields. A question is the utility of the points specifically chosen for the 24-2C relative to the central structural losses that might be expected in glaucoma, which has implications for test location selection.

This study found that half of 24-2C test locations had no colocalized structural and functional defects, as the points fell outside of the area examined in the ganglion cell analysis used for structural correlations (see Limitations). Although the 24-2C is aimed at assessing the central visual field, previous studies comparing 10-2 test locations with the ganglion cell analysis or a similarly small scan zone have also shown that the more peripherally located points do not fall within the scan area[36,37] once ganglion cell displacement had been accounted for.[31]

The macular area has been extensively used as a model for examining the structure-function relationship in glaucoma, especially early in the disease process. Specific

TABLE 3. Comparison of the Ability of Each Test Grid to Identify a Colocalized Functional Defect[a]

	24-2 Only Test Grid			24-2C Test Grid (24-2 Component Only)		
	Yes	No	*P* Value	Yes	No	*P* Value
Functional defects at $P < .05$						
SITA-Standard 24-2 and SITA-Faster 24-2C cohort						
24-2C test grid (24-2 component only)						
Yes	5 (20.8)	3 (12.5)	.6831	7 (30.4)	0 (0)	.1336
No	3 (12.5)	13 (54.2)		4 (17.4)	12 (52.2)	
24-2C test grid (24-2C component)						
Yes	7 (29.2)	1 (4.2)	.3711			
No	4 (16.7)	12 (50.0)				
SITA-Faster 24-2 and 24-2C cohort						
24-2C test grid (24-2 component only)						
Yes	2 (4.4)	6 (13.3)	.7518	5 (11.4)	0 (0)	.0015
No	4 (8.9)	33 (73.3)		12 (27.3)	27 (61.3)	
24-2C test grid (24-2C component)						
Yes	6 (13.3)	2 (4.4)	.0265			
No	11 (24.4)	26 (57.8)				
Functional defects at $P < .01$						
SITA-Standard 24-2 and SITA-Faster 24-2C cohort						
24-2C test grid (24-2 component only)						
Yes	2 (8.3)	4 (16.7)	.7237	5 (21.7)	0 (0)	.0736
No	4 (16.7)	14 (58.3)		5 (21.7)	13 (56.5)	
24-2C test grid (24-2C component)						
Yes	5 (20.8)	1 (4.2)	.2207			
No	5 (20.8)	13 (54.2)				
SITA-Faster 24-2 and 24-2C cohort						
24-2C test grid (24-2 component only)						
Yes	2 (4.4)	4 (8.9)	.3711	3 (6.7)	0 (0)	.0044
No	1 (2.2)	38 (84.4)		10 (22.2)	32 (71.1)	
24-2C test grid (24-2C component)						
Yes	5 (11.1)	1 (2.2)	.0455			
No	8 (17.8)	31 (68.9)				

[a]Table data compare the ability of each test grid to identify a colocalized functional defect (at the $P < .05$ or $P < .01$ level) at a location where a structural defect was identified on the ganglion cell analysis, excluding all locations at which there were no structural losses present. Defect present is indicated by "Yes," and no defect present is indicated by "No." The number of cases is shown with the percentage of total in parentheses. The *P* values for the pairwise McNemar tests are shown.

regions of the macula have been suggested to be particularly vulnerable to early glaucomatous structural loss, for example, the so-called macular vulnerability zone. High-frequency affected locations have served as the basis for other, non-24-2C test grids proposed for adding to the existing 24-2 grid. For example, given the propensity for inferior structural loss to occur in early glaucoma, a focus on points in the superior hemifield has been suggested.

Suggestions for alternative central visual field test grids include customized test grids for the individual patient using either existing perimetric data or adjunctive retinal structure information. Additional test locations can be added or sampled when tested locations in the 24-2 or 10-2 test grid no longer provide useful information, such as when they reach the measurement floor.[38] A focus of this approach would be for longitudinal monitoring, rather than necessarily at the diagnosis stage. Bespoke test grids using retinal structural information can potentially improve structure-function concordance by specifically sampling regions where functional losses are predicted.[39,40] This approach may help to mitigate issues like points 4, 5, 7, 9, and 10 in the present study which, had a no structure-function concordance due to the perimetric test location. A fundamental assumption here, however, is that the retinal structures would form the ground truth. However, depending on the measurement technique, this may preclude cases of glaucoma where functional deficits occur prior to structural loss, detectable using OCT.[41] Finally,

TABLE 4. Number and Proportion of Patients in Whom a Statistically Function Defect or a Structural Defect Was Identified[a]

24-2 Test Locations	SITA-Standard 24-2 and SITA-Faster 24-2C Cohort				SITA-Faster 24-2 and 24-2C Cohort			
	Functional Defects		Structural Defects		Functional Defects		Structural Defects	
Test Location	Defects	*P* Value	Defects, *n* (%)	*P* Value	Defects, *n* (%)	*P* Value	Defects	*P* Value
1 (−3,+3)	7 (17.5)	.2270	19 (47.5)	<.0001	6 (9.4)	.5309	40 (62.5)	<.0001
2 (+3,+3)	3 (7.5)		17 (42.5)		3 (4.7)		20 (31.3)	
3 (−3,−3)	2 (5.0)		15 (37.5)		8 (12.5)		22 (34.4)	
4 (+3,−3)	3 (7.5)		10 (25.0)		3 (4.7)		17 (26.6)	
24-2C Test Locations	Functional Defects		Structural Defects		Functional Defects		Structural Defects	
Test Location	Defects, *n* (%)	*P* Value	Defects, *n* (%)	*P* Value	Defects, *n* (%)	*P* Value	Defects	*P* Value
1 (−5,+1)	6 (15.0)	.6310	20 (50.0)	<.0001	10 (15.6)	.0349	41 (64.1)	<.0001
2 (−1,+5)	5 (12.5)		19 (47.5)		11 (17.2)		40 (62.5)	
3 (+1,+5)	6 (15.0)		18 (45.0)		5 (7.8)		28 (43.8)	
4 (+5,+7)	10 (25.0)		0 (0)		10 (15.6)		0 (0)	
5 (+7,+5)	6 (15.0)		0 (0)		9 (14.1)		0 (0)	
6 (−7,−1)	5 (12.5)		12 (30.0)		7 (10.9)		21 (32.8)	
7 (−7,−5)	7 (17.5)		0 (0)		17 (26.6)		0 (0)	
8 (−1,−5)	6 (15.0)		15 (37.5)		8 (12.5)		26 (40.6)	
9 (+1,−9)	7 (17.5)		0 (0)		16 (25.0)		0 (0)	
10 (+5,−7)	2 (5.0)		0 (0)		5 (7.8)		0 (0)	

[a]Table data show number and proportion of total patients in whom a statistically function defect ($P < .05$ on the Humphrey field analyzer pattern deviation map) or structural defect ($P < .05$ on the ganglion cell analysis deviation map following anatomical correction) was identified at each location for the 24-2 and 24-2C exclusive points for SITA-Standard and SITA-Faster cohorts. *P* values indicate the results of chi-squared tests across test locations for identifying significant differences in proportion.

individual anatomical variations provide a further confounding factor to the deployment of a fixed test grid, especially if only a limited number of locations are added for testing.[42]

As half of the 24-2C exclusive locations did not fall within the ganglion cell analysis ellipse, an alternative model is proposed (Figure 5) where the visual field test grid is corrected for ganglion cell displacement. A fixed arrangement of test locations is proposed that are equidistant based on the underlying anatomical test region. Then, using the displacement of ganglion cells, the correction is reversed to derive the test locations in visual space, that is, Humphrey field analyzer test locations. This framework proposes a more equal spread and greater coverage of test locations within each quadrant of the ganglion cell analysis ellipse, allowing for a uniform assessment of the ganglion cell mosaic in ocular conditions affecting the ganglion cells. In outer retinal diseases, the proposed grid does not need to be corrected for ganglion cell displacement, but rather the regular test grid can be deployed.

• **CLINICAL IMPACT OF 24-2C EXCLUSIVE TEST LOCATIONS:** The present results do not clearly support an increased clinical utility of the 24-2C exclusive test points if significant changes are considered to the management plan achieved using global visual field indices, similar to the work of Wu and associates.[7] Further to the cluster criterion, central defects are often used for identifying advanced glaucoma, and the importance of this distinction is for the purposes of treatment titration. One present issue is the lack of consensus on the significance of central visual field loss, such as how many locations are required to qualify for advanced glaucoma.[43] The contribution of 24-2C specific points to this staging process remains unclear, and further investigations are needed to examine their role in aspects such as quality-of-life and progression analysis

The present results suggest that the current value, comparing the 24-2C grid against the ganglion cell analysis scan pattern, is for specific cases with colocalized sampled structural losses. In patients without these structural losses or where the losses do not reach statistical significance, or where concordance is desirable at specific locations, the value of the 24-2C grid in changing clinical management appears questionable.

• **STUDY LIMITATIONS:** A consecutive recruitment strategy for patients was used in the present study and, as such, did not specifically target patients with central visual field loss. Although this may reduce potential spectrum biases associated with a targeted approached,[44] the entirety of the present cohort did not represent those predicted to have structurally and functionally concordant defects. Individual sample sizes for the SITA-Standard and SITA-Faster cohorts were also smaller than that of Heijl and

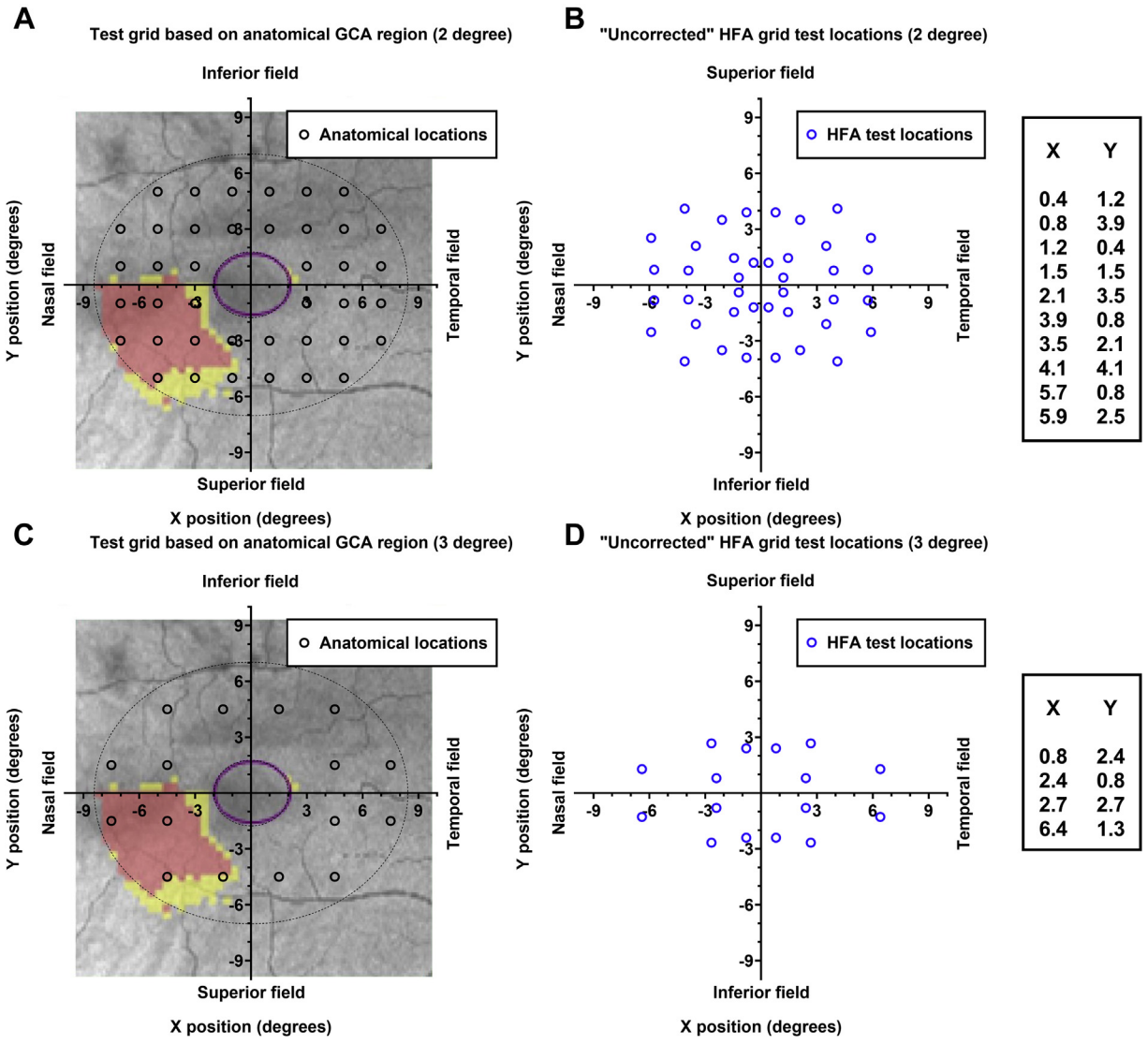

FIGURE 5. A proposed framework for more equal and greater coverage of anatomical regions of interest for the ganglion cell analysis (left panels, black circles) which can then be translated into visual space (e.g., a Humphrey field analyzer grid) for perimetry (right panels, blue circles). (A, B), a grid with 2-degree separation of anatomical test locations (excluding the horizontal and vertical midlines), 40 points. (C, D) a grid with 3° separation of anatomical test locations, totaling 16 points. Cartesian coordinates for visual field test locations (degrees) are shown in the far-right insets.

associates[22] and that of our recent work,[23] so this analysis would benefit from a larger and more diverse cohort.

Also, the 24-2C was tested after the 24-2 test, which may introduce a bias in the form of a fatigue effect. Kelly et al[45] found statistically significant reductions in mean deviation for the second eye tested resulting from fatigue, but this was unlikely to be clinically significant in magnitude. A prediction in this study would be that visual field indices would be systematically worse in the 24-2C. However, aside from mean deviation in SITA-Standard cohort, there were no significant differences in global indices. The shorter test duration afforded by SITA-Faster may be particularly advantageous to mitigate the potential fatigue effect, but this remains to be tested (randomization should be considered in a future study).

False negative and blind spot monitoring using the Heijl-Krakau method for identifying low test reliability results were not used, which may affect the translatability of the present results in some clinical practices. The issue of these reliability indices have been recently discussed,[22] but identification of low test reliability under elevated false negative or blind spot error rates would typically occur in conjunction with patterns of defects observed within the rest of the results.

Ganglion cell analysis printout was chosen for structural analysis as the Cirrus OCT is produced by the same manufacturer as the Humphrey field analyzer. Currently, this structural metric does not provide the option for manual segmentation in clinical practice or delineate the ganglion cell-inner plexiform layer zone, and reports on a limited scan ellipse. As described above (Methods), also, neither the retinal nerve fiber layer scan (optic nerve head scan protocol) nor its combinatory form were incorporated (the Panomap available on the same device). The Panomap has been recently highlighted as potentially useful for understanding patterns of structural progression in glaucoma.[46] Notably, however, the issue of incorporating retinal nerve fiber layer projections in structure-function mapping has been reviewed by Denniss and associates,[33] with limitations to the process, including factors such as the need for additional ocular biometric measurements and high-resolution fiber tracing. There has also been a proposal for localized areas of structure-function correlation using the 10- to 2-degree test grid within the macula, particularly in relation to the more peripheral points.[42] Such peripheral points would correspond to those locations which we found apparently fell outside the ganglion cell analysis printout.

In addition, other OCT scanning protocols such as the macula posterior pole scan (e.g., Spectralis OCT) or widefield scanning incorporating both optic nerve and macula information (e.g., Topcon OCT) may provide additional information with which to perform structure-function correlations.[47] Specifically, widefield protocols providing segmentation information on the same retinal layer throughout the scan may be particularly useful,[35] given that the Cirrus OCT scan protocols yield a truncation between optic nerve and macula scans and thus have data gaps for identifying structure-function agreement. Examination of this problem and incorporation of retinal nerve fiber layer and optic nerve head information to overcome the limited elliptical scan area would be important in a future study.

CONCLUSIONS

ALTHOUGH THE ADDITIONAL TEST POINTS DO NOT change global metrics of visual field measurements, the 24-2C has a notable advantage over the commonly used 24-2 test grid by increasing the sampling of test locations within the central visual field, with only a small increase in test time when using the SITA-Faster algorithm. There is a clinical benefit of additional sampling within the central visual field for identification of defects and correlations with structural findings; however, the implications for disease staging and treatment titration remains the subject of investigation. Structure-function correlations comparing the 24-2C and the ganglion cell analysis using the Cirrus OCT identified half of the test points falling outside the structural scan area and hence are not useful if using this specific scan in clinical practice but suggests the need to integrate a wider or combinatory scan protocol. We also propose a strategy for guiding test point selection for sampling the macular region.

THE AUTHORS HAVE COMPLETED AND SUBMITTED THE ICMJE FORM FOR DISCLOSURE OF POTENTIAL.

Conflicts of Interest and none were reported.

Funding/Support: Guide Dogs NSW/ACT supported the clinical services, enabling data collection for this study and providing support to J.P. and M.K. The funding organization had no role in the design or conduct of this research.

Financial Disclosures: Both authors have reported that they have no relationships relevant to the contents of this paper to disclose.

REFERENCES

1. Jampel HD, Singh K, Lin SC, et al. Assessment of visual function in glaucoma: a report by the American Academy of Ophthalmology. *Ophthalmology* 2011;118(5):986–1002.
2. Phu J, Khuu SK, Yapp M, et al. The value of visual field testing in the era of advanced imaging: clinical and psychophysical perspectives. *Clin Exp Optom* 2017;100(4):313–332.
3. Zeyen TG, Zulauf M, Caprioli J. Priority of test locations for automated perimetry in glaucoma. *Ophthalmology* 1993; 100(4):518–522. discussion 23.
4. Schiefer U, Papageorgiou E, Sample PA, et al. Spatial pattern of glaucomatous visual field loss obtained with regionally condensed stimulus arrangements. *Invest Ophthalmol Vis Sci* 2010;51(11):5685–5689.
5. Heijl A. Perimetric point density and detection of glaucomatous visual field loss. *Acta Ophthalmol (Copenh)* 1993;71(4):445–450.
6. Nouri-Mahdavi K, Mock D, Hosseini H, et al. Pointwise rates of visual field progression cluster according to retinal nerve fiber layer bundles. *Invest Ophthalmol Vis Sci* 2012;53(4): 2390–2394.
7. Wu Z, Medeiros FA, Weinreb RN, Zangwill LM. Performance of the 10-2 and 24-2 visual field tests for detecting central visual field abnormalities in glaucoma. *Am J Ophthalmol* 2018; 196:10–17.
8. Sullivan-Mee M, Karin Tran MT, Pensyl D, et al. Prevalence, features, and severity of glaucomatous visual field loss measured with the 10-2 achromatic threshold visual field test. *Am J Ophthalmol* 2016;168:40–51.
9. Park HY, Hwang BE, Shin HY, Park CK. Clinical clues to predict the presence of parafoveal scotoma on humphrey 10-2 visual field using a humphrey 24-2 visual field. *Am J Ophthalmol* 2016;161:150–159.
10. Odden JL, Mihailovic A, Boland MV, et al. Evaluation of central and peripheral visual field concordance in glaucoma. *Invest Ophthalmol Vis Sci* 2016;57(6):2797–2804.
11. Gillespie BW, Musch DC, Guire KE, et al. The collaborative initial glaucoma treatment study: baseline visual field and

test-retest variability. *Invest Ophthalmol Vis Sci* 2003;44(6):2613–2620.
12. Krupin T, Liebmann JM, Greenfield DS, et al. The Low-pressure Glaucoma Treatment Study (LoGTS) study design and baseline characteristics of enrolled patients. *Ophthalmology* 2005;112(3):376–385.
13. Leske MC, Heijl A, Hyman L, Bengtsson B. Early Manifest Glaucoma Trial: design and baseline data. *Ophthalmology* 1999;106(11):2144–2153.
14. Keltner JL, Johnson CA, Cello KE, et al. Visual field quality control in the Ocular Hypertension Treatment Study (OHTS). *J Glaucoma* 2007;16(8):665–669.
15. Traynis I, De Moraes CG, Raza AS, et al. Prevalence and nature of early glaucomatous defects in the central 10 degrees of the visual field. *JAMA Ophthalmol* 2014;132(3):291–297.
16. Hood DC, Nguyen M, Ehrlich AC, et al. A test of a model of glaucomatous damage of the macula with high-density perimetry: implications for the locations of visual field test points. *Transl Vis Sci Technol* 2014;3(3):5.
17. Tomairek RH, Aboud SA, Hassan M, Mohamed AH. Studying the role of 10-2 visual field test in different stages of glaucoma. *Eur J Ophthalmol* 2019;30:706–713.
18. Blumberg DM, De Moraes CG, Prager AJ, et al. Association between undetected 10-2 visual field damage and vision-related quality of life in patients with glaucoma. *JAMA Ophthalmol* 2017;135(7):742–747.
19. Fung SS, Lemer C, Russell RA, et al. Are practical recommendations practiced? A national multi-centre cross-sectional study on frequency of visual field testing in glaucoma. *Br J Ophthalmol* 2013;97(7):843–847.
20. Ehrlich AC, Raza AS, Ritch R, Hood DC. Modifying the conventional visual field test pattern to improve the detection of early glaucomatous defects in the central 10 degrees. *Transl Vis Sci Technol* 2014;3(6):6.
21. Chen S, McKendrick AM, Turpin A. Choosing two points to add to the 24-2 pattern to better describe macular visual field damage due to glaucoma. *Br J Ophthalmol* 2015;99(9):1236–1239.
22. Heijl A, Patella VM, Chong LX, et al. A New SITA Perimetric Threshold Testing Algorithm: Construction and a Multicenter Clinical Study. *Am J Ophthalmol* 2019;198:154–165.
23. Phu J, Khuu SK, Agar A, Kalloniatis M. Clinical evaluation of Swedish interactive thresholding algorithm-faster compared with Swedish interactive thresholding algorithm-standard in normal subjects, glaucoma suspects, and patients with glaucoma. *Am J Ophthalmol* 2019;208:251–264.
24. Mills RP, Budenz DL, Lee PP, et al. Categorizing the stage of glaucoma from pre-diagnosis to end-stage disease. *Am J Ophthalmol* 2006;141(1):24–30.
25. Huang J, Hennessy MP, Kalloniatis M, Zangerl B. Implementing collaborative care for glaucoma patients and suspects in Australia. *Clin Exp Ophthalmol* 2018;46(7):826–828.
26. Phu J, Khuu SK, Agar A, et al. Visualising the consistency of clinical characteristics that distinguish healthy, suspect and manifest glaucoma patients. *Ophthalmol Glaucoma* 2020;3(4):274–287.
27. Prum BE Jr, Rosenberg LF, Gedde SJ, et al. Primary open-angle glaucoma preferred practice pattern guidelines. *Ophthalmology* 2016;123(1):P41–P111.
28. Phu Jack, Kalloniatis Michael. A strategy for seeding point error assessment for retesting (SPEAR) in perimetry applied tonor-mal, suspect and glaucoma patients. *American Journal of Ophthalmology* 2020; https://doi.org/10.1016/j.ajo.2020.07.047. In press.
29. Hood DC, Kardon RH. A framework for comparing structural and functional measures of glaucomatous damage. *Prog Retin Eye Res* 2007;26(6):688–710.
30. Tong J, Phu J, Khuu SK, et al. Development of a spatial model of age-related change in the macular ganglion cell layer to predict function from structural changes. *Am J Ophthalmol* 2019;208:166–1177.
31. Drasdo N, Millican CL, Katholi CR, Curcio CA. The length of Henle fibers in the human retina and a model of ganglion receptive field density in the visual field. *Vision Res* 2007;47(22):2901–2911.
32. Yoshioka N, Zangerl B, Phu J, et al. Consistency of structure-function correlation between spatially scaled visual field stimuli and in vivo OCT ganglion cell counts. *Invest Ophthalmol Vis Sci* 2018;59(5):1693–1703.
33. Denniss J, Turpin A, McKendrick AM. Relating optical coherence tomography to visual fields in glaucoma: structure-function mapping, limitations and future applications. *Clin Exp Optom* 2019;102(3):291–299.
34. Lamparter J, Russell RA, Zhu H, et al. The influence of inter-subject variability in ocular anatomical variables on the mapping of retinal locations to the retinal nerve fiber layer and optic nerve head. *Invest Ophthalmol Vis Sci* 2013;54(9):6074–6082.
35. Hood DC, Tsamis E, Bommakanti NK, et al. Structure-function agreement is better than commonly thought in eyes with early glaucoma. *Invest Ophthalmol Vis Sci* 2019;60(13):4241–4248.
36. Sato S, Hirooka K, Baba T, et al. Correlation between the ganglion cell-inner plexiform layer thickness measured with cirrus HD-OCT and macular visual field sensitivity measured with microperimetry. *Invest Ophthalmol Vis Sci* 2013;54(4):3046–3051.
37. Raza AS, Cho J, de Moraes CG, et al. Retinal ganglion cell layer thickness and local visual field sensitivity in glaucoma. *Arch Ophthalmol* 2011;129(12):1529–1536.
38. Turpin A, Morgan WH, McKendrick AM. Improving spatial resolution and test times of visual field testing using AR-REST. *Transl Vis Sci Technol* 2018;7(5):35.
39. Montesano G, Rossetti LM, Allegrini D, et al. Improving visual field examination of the macula using structural information. *Transl Vis Sci Technol* 2018;7(6):36.
40. Ballae Ganeshrao S, Turpin A, Denniss J, McKendrick AM. Enhancing structure-function correlations in glaucoma with customized spatial mapping. *Ophthalmology* 2015;122(8):1695–1705.
41. Banitt MR, Ventura LM, Feuer WJ, et al. Progressive loss of retinal ganglion cell function precedes structural loss by several years in glaucoma suspects. *Invest Ophthalmol Vis Sci* 2013;54(3):2346–2352.
42. Turpin A, Chen S, Sepulveda JA, McKendrick AM. Customizing structure-function displacements in the macula for individual differences. *Invest Ophthalmol Vis Sci* 2015;56(10):5984–5989.
43. Peters D, Bengtsson B, Heijl A. Threat to fixation at diagnosis and lifetime risk of visual impairment in open-angle glaucoma. *Ophthalmology* 2015;122(5):1034–1039.
44. Ransohoff DF, Feinstein AR. Problems of spectrum and bias in evaluating the efficacy of diagnostic tests. *N Engl J Med* 1978;299(17):926–930.
45. Kelly SR, Bryan SR, Crabb DP. Does eye examination order for standard automated perimetry matter? *Acta Ophthalmol* 2019;97(6):e833–e888.

46. Lee WJ, Na KI, Ha A, et al. Combined use of retinal nerve fiber layer and ganglion cell-inner plexiform layer event-based progression analysis. *Am J Ophthalmol* 2018;196:65–71.

47. Brandao LM, Ledolter AA, Schotzau A, Palmowski-Wolfe AM. Comparison of two different OCT systems: retina layer segmentation and impact on structure-function analysis in glaucoma. *J Ophthalmol* 2016;8307639.